Physics – Uspekhi **39** (5) 539 – 544 (1996)

FROM THE HISTORY OF PHYSICS PACS numbers: **28.70.+y**, **47.40.–x**, 62.20.Fe

Explosive laboratory devices for shock wave compression studies

L V Al'tshuler, R F Trunin, K K Krupnikov, N V Panov

Contents

Abstract. History of creation and schemes of Arzamas-16 explosive laboratory devices for dynamical compressibility measurements at pressures up to 2 – 2.5 TPa are described, in which a thin, metallic impactor of spherical geometry is accelerated by the explosion products in converging detonation waves. The iron shock adiabat obtained with these devices over the period from 1948 to the early 60s and used as a dynamical standard in megabar and terapascal compressibility studies of other substances, is presented. In deriving its parameters for up to 10 TPa, iron compressibility data from underground nuclear explosions of the 70s, and calculated results from the modified quantum-statistical model have been employed.

1. Introduction

Dynamical compressibility measurements at pressures of several tens of GPa were conducted at the Los-Alamos Laboratory since 1945 and widely published beginning the mid-50s [1 – 3]. In the Russian Federal Nuclear Centre (Arzamas-16), systematic studies were initiated independently in 1948, and already the earliest reports about that work (later in [4,5]) contained data on then huge pressures of 400 GPa. By the early 60s, these pioneering results were refined [6], and the laboratory pressure range was extended up to $\sim$ 1000 GPa (10 Mbar) [7 – 9]; today, the upper pressure limit is close to 2500 GPa [10, 11].

In the USA, specimen impact pressures of order 500 GPa were achieved by using two-stage light-gas artillery systems — guns — which impart the impactor to maximum velocities of about 8 km s^{-1} [12, 13].

As to the Russian ultrahigh pressure experiments [4 – 11], the interested reader was to be content solely with low-informative assertions of the type "... 400-GPa pressures were attained using steel impactors at 9.1 km s^{-1}" [6] or "... a cumulative device was used, in which the products of the explosion of high-power explosive propel a steel impactor (a specially shaped liner) to a velocity of 18.5 km s^{-1}" [10]. The scarcity of experimental information on the Russian ultrahigh pressure studies was noted, in particular, in a 1988 Livermore National Laboratory paper [14] on ultrahigh pressure physics of metals. In its authors' words, "... the compressibility data of Kormer et al. [8] and Al'tshuler, Bakanova, and Trunin [7] on copper and lead near 10 Mbar are obtained using unknown shock pressure generators and have not yet been reproduced". The situation is much the same today.

The experimental devices developed in the Russian Federal Nuclear Centre (Arzamas-16) will be discussed in terms of the absolute compressibility measurement with the dynamic standard (Fe) using the 'braking' technique [4, 15]. It will be reminded that the quantities measured in this approach are the impactor velocity W, and the shock wave velocity D in a fixed target of the same material as the impactor. At the collision, the interface symmetry condition implies that the mass velocity behind the shock wave front in such a target is $U = (1/2)W$. By the conservation laws at the shock wave discontinuity surface, the fixed values of U and D determine the thermodynamic parameters of the compressed state. The pressure attained in the standard material (iron, in our case) is the basic characteristic of the explosive laboratory devices we are considering. For a plane geometry and normal detonation regimes, it is found [6, 15] that plates accelerated by the explosion products acquire velocities of $\sim$ 6 km s^{-1}, and pressure in iron targets is $\sim$ 200 GPa.

Much larger shock wave amplitudes were realised with explosive measurement systems using convergent over-com-

L V Al'tshuler Pulsed Thermal Physics Research Centre at the Institute for High Temperatures, Russian Academy of Sciences
ul. Izhorskaya 13/19, 127412 Moscow, Russia
Tel. (7-095) 485 79 88
Fax (7-095) 485 79 90
K K Krupnikov All-Russian Research Institute of Technical Physics (VNIITF), Snezhinsk, Chelyabinsk Region, Russia
Tel. (7-8351) 723 11 27
Fax (7-8351) 723 01 25
E-mail: shor@gdd.ch70.chel.su
N V Panov, R F Trunin All-Russian Research Institute of Experimental Physics (VNIIEF), 607200 Sarov (Arzamas-16), Nizhniĭ Novgorod Region, Russia
Fax (7-83130) 545 65

Received 21 Junuary 1996
Uspekhi Fizicheskikh Nauk **166** (5) 575 – 581 (1996)
Translated by E G Strel'chenko; edited by A Radzig

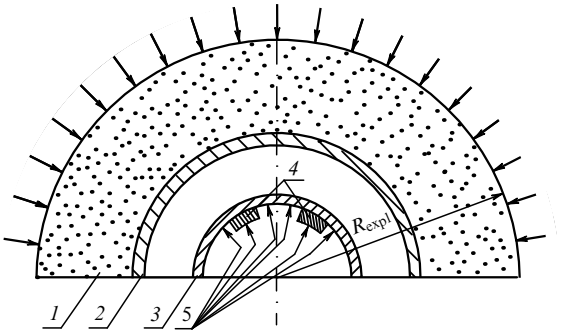

Figure 1. Schematic diagram of BM and IC devices: *1* — hemispherical explosive charge; *2* — shell (Fe); *3* — screen (Fe); *4* — specimens under study; *5* — electrical pin contactors for shock wave velocity (D) measurements.

pressed detonation waves. For a spherical geometry, the detonation wave front pressures grow continually towards the centre. Therefore, in the arsenal of dynamical methods, the hemispherical charge simultaneously primed on its outer surface is an ideal tool for studying materials at ultrahigh pressures.

The schematic diagram of the measuring device developed for this purpose is shown in Fig. 1. This is a hemispherical charge containing an inner recess into which a thin-walled metallic (steel) shell is inserted. When acted upon by the explosion products in the convergent detonation wave, the shell-impactor is accelerated ('converges') to the centre of the device, its velocity being increased with decreasing radius. Placing targets (screened specimens) at different depths (radii) allows different pressures up to 10 – 20 Mbar to be achieved in their bulks. While the braking method basically has no pressure limitations, at the interpretation stage the following features of the spherical experiment must be taken into consideration:

— the relation $U = (1/2)W$ is exact at the impact surface, i.e. for screen radius r_s exceeding the radius r_m of the specimen wave velocity measurement [15]. However, as hydrodynamical iron shell – iron target impact analyses have repeatedly shown, the convergence increases virtually to the same extent the 'free run' iron-shell velocity $W(r)$, and the mass velocity behind the shock front in the iron screens and iron specimens. We therefore assume that the mass velocity at r_m is also $U(r_m) = (1/2)W(r_m)$;

— as the convergent detonation wave reflects from the shell, irreversible shock heating takes place at the shell position radius. As a consequence, in cascade acceleration systems a few percent difference between $W/2$ and U forms (see below);

— at the large gauge length S of velocity measurement, the average wave velocity $\bar{D}$ recorded in the specimen may differ from the local velocity $D(r_m)$ at the nominal radius r_m in the middle of the specimen. In tabulating experimental data, both the average $\bar{D}$ and the corrected $D(r_m)$ are indicated.

Scanty information on dynamical experiments using shell acceleration by the explosion products in convergent spherical detonation waves was first given in a 1962 British publication [16]. There was no further development of this method abroad.

In the following sections we describe the Russian Federal Nuclear Centre measuring devices which have provided impact compressibility and equations-of-state information for a number of substances in the pressure range 200 to 2500 GPa. For all variants investigated, major geometrical parameters and dynamic characteristics are tabulated, which include the relative radii r_{sh} and thicknesses Δ_{sh} of the shells and the relative radii r_s of the screens; wave velocity gauge lengths S; free-run shell velocities $W(r_m)$ over measurement radii r_m; shock wave mass velocities $U(r_m)$ in iron specimens; the average $\bar{D}$ and local $D(r_m)$ wave velocities; and, finally, the thermodynamical parameters of compressed states of iron (compression ratio $\sigma = \rho/\rho_0$ and pressure P) as calculated from the conservation laws for shock wave discontinuity surfaces. The last column lists references, the '+' sign indicating that the present is the first publication of the result. The probable measurement error is about 1 – 1.5% for mass and wave velocities, and 1.5 – 2% for pressure.

2. BM devices for producing pressures of 200 – 400 GPa in iron

The hemispherical measuring device described above (Fig. 1) has come to be known as the 'Big Model' and was developed by L V Al'tshuler, E I Zababakhin, Ya B Zel'dovich, and K K Krupnikov [17, 4] along with V I Zhuchikhin, B N Ledenev, and M I Brazhnik [4]. Already back in 1948 devices of this type yielded impact compression ratios for iron, uranium and other metals at $P \sim 400$ GPa. Later, to compare plane geometry [6, 15] and spherical data, a relatively slow IC ('intermediate charge') model was developed. The major geometrical parameters and dynamical characteristics of these two devices are listed in Table 1. Analysis shows that, for similar pressures, IC data are in good agreement with 'plane' experiments. It is to be noted that, for both devices, the calculated corrections to D are negligible and those to U are insignificant. The impact compression ratios obtained with the BM charge yielded the position of the standard iron adiabat at these pressures, which was used for measuring the impact compressibility of other metals by the reflection technique [5].

In 1966, the results for gold [5] and tungsten [18] were confirmed [12] by precision experiments on pneumatic measuring systems.

3. Devices for producing pressures of 300 – 900 GPa in iron

The SC ('soft charge') devices developed in the late 50s by L V Al'tshuler, A A Bakanova, and R F Trunin [6, 7] made the measurements more accurate and easier to interpret and more than doubled the pressure range (to 900 GPa). The latter goal

Table 1. Parameters and dynamic characteristics of IC and BM devices

Device	r_{sh}	Δ_{sh}, mm	r_m	$W(r_m)$, km s^{-1}	$U(r_m)$, km s^{-1}	r_s	S, mm	$\bar{D}$, km s^{-1}	$D(r_m)$, km s^{-1}	σ	P, GPa	Ref.
IC	0.40	6.6	0.170	6.20	3.08	0.197	4	8.78	8.78	1.540	210	+
BM	0.40	4.8	0.137	8.64	4.26	0.177	8	10.67	10.67	1.664	357	[6]

was achieved by taking thinner shells and placing the target specimens at smaller radii. To improve the symmetry of the convergent detonation waves, better synchronisation of surface charge priming, and explosives of more homogeneous composition were employed. This made the motion of the shells and shock waves in the target more symmetrical which, in turn, made it possible, with no loss in accuracy, to decrease specimen thickness, and hence to reduce corrections for convergence.

The next step was to lower the shock-induced shell heating. This was achieved by allowing small air clearances between the shell and the explosive. This method of reducing pressures (and hence temperatures) was suggested by E I Zababakhin and Ya B Zel'dovich.

The schematic diagram of an air-clearance SC measuring device is shown in Fig. 2. A number of SC versions have been developed (see Table 2). One group of them involves a shell thickness of $\Delta_{sh} \simeq 3$ mm and an air clearance of 12 mm. Devices of this group differ in target position radii and hence in measurement radii: $r_m = 0.186$, 0.132, and $0.07R_{expl}$. In accordance with the pressures attained at these radii, the charges were called SC-3, SC-3.5, SC-4, and SC-8-1 [here 3, 3.5, 4, and 8 being the pressures (in Mbars) in iron in these devices].

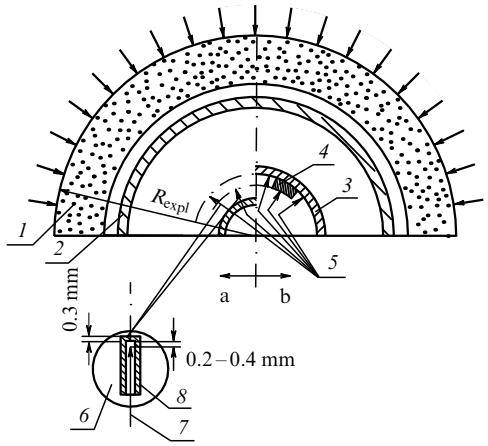

Figure 2. Schematic diagram of a SC device for measuring (a) shell flight velocity, and (b) shock wave velocity in specimens: *1–5* — see caption to Fig. 1; *6* — electrical pin contactors for recording shell flight velocity W; *7* — copper pin; *8* — steel cover plate.

In SC-8-2 and SC-9, thinner ($\Delta_{sh} = 1.5$ mm) iron shells with a 9-mm air clearance above them were used. Measurements were carried out at $r_m = 0.08$ and $0.07R_{expl}$, and the iron pressures detected were 780 and 860 GPa.

The effect of the air clearance on shock wave formation in shells at $r_{sh} = 0.35R_{expl}$ was examined by Zubarev and Panov using the electromagnetic method described in [19]. It is found that if the air clearance is 3–5 shell thicknesses, the shock wave intensity in the shell is roughly halved: the reason in fact for allowing clearances into the SC scheme. Incident-shock shell pressures were assessed from the fly-away indicator velocity using the electrical pin-contactor and photochronographic techniques. The pressures obtained ($P \approx 45$ GPa) do not deviate much from the plate pressures due to an incident plane detonation wave. Nor, naturally, does the aftershock shell heating exceed the corresponding plate heating ($T \sim 700\,^{\circ}$C).

A word now about the symmetry of shell motion over the measurement radii. Clearly, the degree of spherical symmetry of this motion determines the reliability and reproducibility of the results. The symmetry of the motion was determined by photochronography at radii close to those used in measuring shock wave parameters. The spread (asymmetry) in the shell's arrival time at the target was $\Delta t \leqslant 6 \times 10^{-8}$ s over the entire zone free of unloading waves propagating from the explosive charge base perimeter.

Similar asymmetries resulted from shock wave passage through steel plates covering the upper target electrical pin contactors. Clearly, the time spread values cited indicate that the motion of the impactor and of the waves in the targets is not symmetrical enough to permit single-run compressibility measurements. Therefore, the practical data processing approach we came to was that each experimental point, i.e. each D and $W = 2U$ pair, was taken to be the mean of 4–6 independent measurements.

Motion parameters — the shell velocity W and the wave velocity in the target D — were determined for a number of different target location radii. For $r_m = 0.186$, 0.132, and $0.08R_{expl}$, both D and W were recorded; in two cases (SC-8-1 and SC-9) wave velocities were measured at $r_m = 0.07R_{expl}$, whereas W was measured at $r = 0.08R_{expl}$. W at $r_m = 0.07R_{expl}$ can hardly be recorded with a required accuracy because of there being no sufficient place for the pins to function independently. The $r_m = 0.07R_{expl}$ result in this case was calculated from the shell convergence law. This did not add any significant errors according to our estimates.

W and D were measured by locating electrical pin contactors on the shell trajectory (Fig. 2) or on that of the shock wave in the target.

SC data on iron are listed in Table 2.

4. Cascade measuring devices for producing pressures from 900 to 1300 GPa

Pressures close to 10 Mbar were first obtained in the Russian Federal Nuclear Centre (Arzamas-16) in 1951 by the use of a

Table 2. Parameters and dynamic characteristics of SC devices

Device	r_{sh}	Δ_{sh}, mm	r_m	$W(r_m)$, km s^{-1}	$U(r_m)$, km s^{-1}	r_s	S, mm	$\bar{D}$, km s^{-1}	$D(r_m)$, km s^{-1}	σ	P, GPa	Ref.
SC-3	0.35	3.08	0.186	7.21	3.61	0.21	4	9.69	9.69	1.595	275	+
SC-3.5	0.30	3.08	0.132	8.30	4.15	0.159	4	10.58	10.58	1.645	345	+
SC-4	0.35	3.08	0.132	9.10	4.55	0.159	4	11.26	11.26	1.678	400	[6]
SC-8-1*	0.35	3.08	0.07	14.0*	7.00	0.097	4	14.64	14.53	1.927	800	+
SC-8-2	0.30	1.5	0.08	13.80	6.90	0.088	4	14.45	14.35	1.926	780	+
SC-9	0.30	1.5	0.07	14.68	7.34	0.088	4	15.15	14.93	1.967	860	[7]

* Shell flight velocity W is measured at $r_m = 0.08$. Transformation to $r_m = 0.07$ is carried out via the calculated shell convergence law.

'cascade hemispherical' device. These studies were performed by K K Krupnikov and M I Brazhnik [9] using the scheme proposed by L V Al'tshuler. Earlier, in 1948, the principle of one-dimensional multicascade plate acceleration had been analysed and justified by E I Zababakhin (see [20]). According to the scheme shown in Fig. 3, a 'thick' plate, having been accelerated to W_1 by the explosion products of the first charge, strikes charge *2* and produces in it an overcompressed detonation wave, whose explosion products expand to accelerate to $W_2 > W_1$ a thinner plate in contact with charge *2*. The acceleration process may be continued to the third cascade and beyond. This approach has been employed for the high-velocity acceleration of molybdenum foils [21] and thin copper plates [22]. For thicknesses 0.5 and 0.1 mm, the plates gained velocities of 9.1 and 11.3 km s^{-1}, respectively [23]. Thin foils, however, necessarily require small gauge length measurements (i.e. ones outside the zone of influence of the unloading waves reflected from the rear surface of the striking foil), which, given the existing asymmetry conditions, increased kinematic parameter errors beyond the usually accepted tolerance.

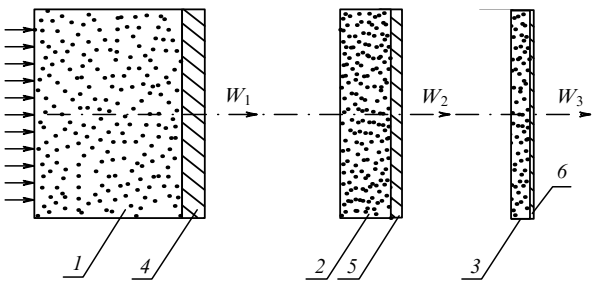

Figure 3. Schematic diagram of one-dimensional multicascade plate acceleration: *1–3* — explosive charges of the first, second, and third cascades; *4–6* — plates of the first, second, and third cascades.

The geometrical parameters and dynamical characteristics of cascade shots in spherical geometry are shown in Fig. 4 and listed in Table 3. The first cascade is a BM one, into which a second cascade, a layer of explosive with a 2-mm steel shell in contact with its inner side, is built in. In two-cascade TC-9 and TC-9-1 devices, the shell velocity at the measurement radius $r_m = 0.068R_{expl}$ was 15.7 ± 0.2 km s^{-1} and the recorded pressure, 910 ± 20 GPa.

The extension of the pressure range to 1350 GPa was achieved with the same type of device (TC-13) by reducing the measurement radius to $r_m = 0.045R_{expl}$. The results of these 1956–1957 experiments were published in [24]. The motion asymmetry of the second cascade shell in this device was $\Delta t \leqslant 7 \times 10^{-8}$ s. Through a series of experiments, the shock wave velocity in iron was found to be $D = 18.67$ km s^{-1}. However, thicker (12-mm) specimens, led to larger convergence corrections, down to -5% in this case.

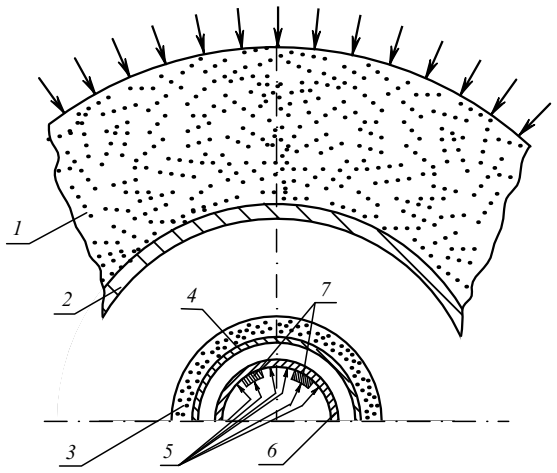

Figure 4. Schematic diagram of a two-cascade hemispherical device: *1, 3* — explosive charges of the first and second cascades; *2, 4* — the shells of the first and second cascades; *5* — same as in Fig. 1; *6* — cover plate (Fe); *7* — specimens under study.

The second parameter, the shell velocity at the measurement radius, was taken from the $W(r)$ curve calculated for the second cascade shell. The calculation was checked by comparing the theoretical and experimental results for total times of shell flight from the inner shell boundary (at initial position) to three different radii (the last one exceeding the measurement radius). On the average, good agreement between theory and experiment was found.

The experiments also involved the correction for the heating of the second cascade shell (wave amplitude 200 GPa); its (negative) value was 3%. The TC-13 iron compression parameters so corrected are summarised in Table 3.

Two factors cast shadow on the accuracy of the data obtained with this technique:

— large convergence corrections and the heating of the second cascade shell, and

— using W derived from a computed dependence, and the integral (time-of-flight based) experimental check of the latter. One cannot rule out that in actual fact the velocity of the shell — that is, its differential characteristic — may differ from that calculated.

The results obtained are at the limit of capability of such systems because at smaller radii measuring kinematic parameters with desired accuracy is difficult, and corrections for convergence are too large.

The extension to higher pressures became possible only after the iron shock adiabat had been determined in underground explosion experiments [25–27]. From these, the iron shock adiabat for pressures of up to 10 TPa (100 Mbar) was obtained. This naturally simplified the situation. Today, whatever of the new terapascal devices is employed, the initial

Table 3. Two-cascade measuring devices

Device	r_{sh}	Δ_{sh}, mm	r_m	$W(r_m)$, km s^{-1}	$U(r_m)$, km s^{-1}	r_s	S, mm	$\bar{D}$, km s^{-1}	$D(r_m)$, km s^{-1}	σ	P, GPa	Ref.
TC-9	0.4/0.183	4.8/2	0.068	15.47	7.52	0.096	11.0	15.50	15.16	1.985	894	[9]
TC-9-1	0.4/0.183	4.8/2	0.068	15.87	7.71	0.093	10.5	15.80	15.50	1.990	938	[9]
TC-13	0.4/0.183	4.8/2	0.045	19.96	9.70	0.075	12.0	18.67	17.74	2.206	1350	[24]

parameters can be determined by simply measuring the shock wave velocity in standard iron and then employing its $D(U)$ dependence to find the corresponding mass velocity U. The method of reflection then allows compressibility measurements for any substances to be performed without measuring the impactor velocity.

5. Iron shock adiabat

Previous laboratory experiments (see Tables 1 – 3) yielded the Hugoniot adiabat of the high-pressure phase of iron in the interval from 9.35 to 1.3 TPa. In this interval, the adiabat is satisfactorily described by the $D(U)$ relation proposed in 1981 in Ref. [24]. For $P \sim 0.9$ TPa, this relation is confirmed by SC-8 and SC-9 measurements. The underground results of Refs [25 – 27] reproduced in Table 4 cover the terapascal shock pressure range from 4.1 to 10.5 TPa.

Table 4. Underground iron shock compression results

U, km s^{-1}	D, km s^{-1}	σ	P, TPa	Ref.
18.25	28.85	2.73	4.13	[25, 27]
21.35	32.46	2.93	5.42	[25, 27]
30.60	43.50	3.37	10.50	[26, 27]

In total, the experimental impact compressibility data for iron can be approximated by the following three quadratic relations:

$$D_1 = 3.664 + 1.79U - 0.0342U^2\,,$$
$$1.4\ \text{km s}^{-1} < U < 8\ \text{km s}^{-1}\,; \qquad (1)$$
$$D_2 = 5.869 + 1.239U + 0.00017U^2\,,$$
$$8\ \text{km s}^{-1} < U < 22\ \text{km s}^{-1}\,; \qquad (2)$$
$$D_3 = 6.982 + 1.190U + 0.00011U^2\,,$$
$$U > 22\ \text{km s}^{-1}\,, \qquad (3)$$

which have identical derivatives for $U = 8$ km s^{-1} ($P = 0.99$ TPa) and $U = 22$ km s^{-1} ($P = 5.7$ TPa). For $P \geqslant 5.7$ TPa, the adiabat (3) merges into the Hugoniot adiabat as obtained by the quantum-statistical analysis of Kalitkin [28] including the Kopyshev nuclear interaction [29].

The adiabat of iron specified by the $D(U)$ dependences above is plotted on the semilog scale $\log P - \sigma$ in Fig. 5, and in the $D-U$ variables, in Fig. 6. The individual experimental points fall to the interpolation curves to within $D \sim 100-150$ m s^{-1} in D variable, which may be considered satisfactory.

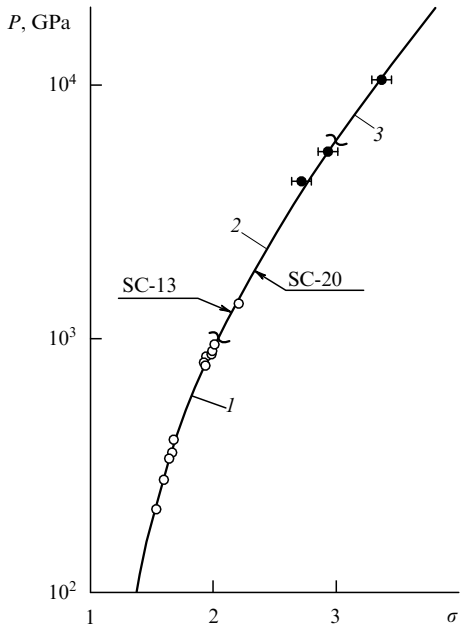

Figure 5. Iron Hugoniot adiabat: *1* — calculated from (1); *2* — calculated from (2); *3* — calculated from (3), ○ — experimental data (from Tables 1 – 3), • — underground explosion data (Table 4). SC-13 and SC-20 device parameters are shown in Table 5.

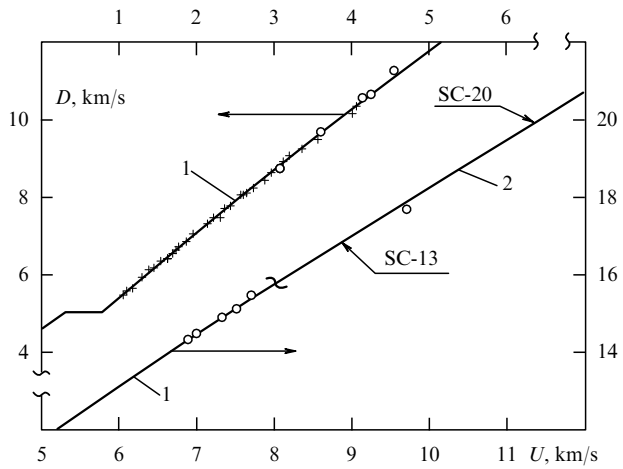

Figure 6. $D-U$ diagram of Fe: ○, *1, 2* — same as in Fig. 5; + — data from Ref. [31].

6. New laboratory measurements in the terapascal range

Knowing the iron Hugoniot adiabat in the terapascal range has extended the range of laboratory impact compressibility studies up to ~ 2.5 TPa. In hemispherical measuring devices developed for this purpose [10, 11], standard dynamic characteristics were derived from the shock wave velocities in iron specimens positioned at radii $0.05R_{\text{expl}}$ (SC-13) and $0.04R_{\text{expl}}$ (SC-20).

The hemispherical charge in these devices was made of compressed RDX-based substance, had an outer radius of about 1.5 times that of the previous SC charges, and provided a somewhat better shock wave symmetry in the specimens. The air clearance above the shell was 11 mm. As in other specimens of this type, the temperature corrections due to the incident-shock shell heating were neglected in interpreting experimental data.

The parameters of the SC-13 and SC-20 devices and the pressures measured in standard specimens over the range 1.2 – 1.8 TPa are given in Table 5, and the experimental results [10, 11] on the impact compressibility of some metals, in Table 6.

The pressures for molybdenum given in Table 6 exceed those obtained from the underground nuclear explosion

Table 5. Parameters and characteristics of terapascal measuring devices

Device	r_{sh}	Δ_{sh}, mm	r_m	r_s	S, mm	$D(r_m)$, km s^{-1}	$U(r_m)$, km s^{-1}	σ	P, TPa	Ref.
SC-13	0.4	3	0.05	0.068	4	17.35	9.26	2.145	1.26	[10, 11]
SC-20	0.4	3	0.04	0.057	4	20.19	11.54	2.334	1.83	

Table 6. Measured SC-13 and SC-20 compressibilities of some metals

Device	Metal	$D(r_m)$, km s^{-1}	$U(r_m)$, km s^{-1}	σ	P, TPa	Comment
SC-13	Al	20.9	12.20	2.40	0.69	Compression parameters are calculated from the initial states of the standard metal (Fe) in the devices SC-13 and SC-20 from Table 5.
	Ta	13.3	7.48	2.285	1.66	
SC-20	Al	24.17	15.08	2.659	0.99	
	Ti	20.95	13.67	2.878	1.290	
	Mo	18.74	10.74	2.342	2.050	
	Ta	15.85	9.36	2.442	2.470	

experiments on the same metal [30]; for tantalum, the record values of the parameters at hand were reached.

7. Conclusions

Further extension of the experimental range may be achieved by using much larger explosive charges, by adding a second cascade, reducing measurement radii, and, finally, by taking more powerful explosives. This, of course, will require new technologies and procedures at all preparation and performance stages of laboratory measurements, but the labour-consuming and costly research along these lines will apparently be low effective since the expected shell flight velocity increase is estimated to be 15 – 20% or less.

Acknowledgments

We consider it our obligation to mention that a valuable contribution to the development of dynamic methods was made by A A Bakanova (1921 – 1979), a member of our Laboratory since its formation, and for two decades the leading specialist in this line of research. Important contributors to the pioneering studies of the shock compressibility of metals are V I Zhuchikhin, B N Ledenev, and M I Brazhnik, and, at various stages of dynamic research, I P Dudoladov, M V Zhernokletov, V N Zubarev, M N Pavlovskiĭ, G V Simakov, A I Funtikov, and research team leaders, V A Tsukerman and S B Kormer.

The experimental work in the Russian Federal Nuclear Centre (Arzamas-16) was conducted in close cooperation with theorists in a creative atmosphere established by the Academicians Ya B Zel'dovich, E I Zababakhin, A D Sakharov, and the scientific leader of the Centre, Academician Yu B Khariton. The unique conditions for scientific work set up in the Arzamas Centre allowed record results to be achieved in a number of directions of experimental physics.

References

1. Walsh J M, Christian R H *Phys. Rev.* **97** (6) 1544 (1955)
2. Goranson R W et al. *J. Appl. Phys.* **26** (12) 1472 (1955)
3. Walsh J M et al. *Phys. Rev.* **108** (2) 196 (1957)
4. Al'tshuler L V et al. *Zh. Eksp. Teor. Fiz.* **34** (4) 874 (1958) [*Sov. Phys. JETP* **34** 606 (1958)]
5. Al'tshuler L V, Krupnikov K K, Brazhnik M I *Zh. Eksp. Teor. Fiz.* **34** 886 (1958) [*Sov. Phys. JETP* **34** 614 (1958)]
6. Al'tshuler L V et al. *Zh. Eksp. Teor. Fiz.* **38** 790 (1960) [*Sov. Phys. JETP* **11** 573 (1960)]
7. Al'tshuler L V, Bakanova A A, Trunin R F *Zh. Eksp. Teor. Fiz.* **42** 91 (1962) [*Sov. Phys. JETP* **15** 65 (1962)]
8. Kormer S B et al. *Zh. Eksp. Teor. Fiz.* **42** 686 (1962) [*Sov. Phys. JETP* **15** 477 (1962)]
9. Krupnikov K K et al. *Dokl. Akad. Nauk SSSR* **148** 1302 (1963) [*Sov. Phys. Dokl.* (1963)]
10. Trunin R F, Panov N V, Medvedev A B *Teplofiz. Vys. Temp.* **33** 329 (1995)
11. Trunin R F, Panov N V, Medvedev A B *Pis'ma Zh. Eksp. Teor. Fiz.* **62** 572 (1995) [*JETP Lett.* **62** 591 (1995)]
12. Jones A H, Isbell W M, Maiden C J *J. Appl. Phys.* **37** (9) 3493 (1966)
13. Mitchel A C, Nellis W J *J. Appl. Phys.* **52** (5) 3363 (1981)
14. Nellis W J et al. *Phys. Rev. Lett.* **60** (14) 1414 (1988)
15. Al'tshuler L V *Usp. Fiz. Nauk* **85** 197 (1965) [*Sov. Phys. Usp.* **8** 52 (1965)]
16. Skidmore I C, Morris E, in *Proc. Symp. Thermodynamics of Nuclear Materials, Vienna, 1962* (Vienna: IAEA, 1962) p. 173
17. Khariton Yu B, Smirnov Yu N "The Khariton Version" *Bull. Atomic Scientists* **5** 20 (1995)
18. Krupnikov K K, Brazhnik M I, Krupnikova V P *Zh. Eksp. Teor. Fiz.* **42** 675 (1962) [*Sov. Phys. JETP* **15** 470 (1962)]
19. Zaĭtsev V M, Pokhil P F, Shvedov K K *Dokl. Akad. Nauk SSSR* **132** 1339 (1960) [*Sov. Phys. Dokl.* (1960)]
20. Al'tshuler L V, in *Khochesh Mira — Bud' Sil'nym* (If You Want Peace, be Strong) (Arzamas-16: VNIIEF, 1996)
21. Ternovoi V Ya, in *Nestatsionarnye Problemy Gidrodimamiki* (Dinamika Sploshnoĭ Sredy, v. 48) [Nonstationary Problems in Hydrodynamics (Dynamics of Continua, No. 48)] (Novosibirsk: Institute of Hydrodynamics of the Siberian Branch of the Academy of Sciences of the USSR, 1980) p. 141
22. Ivanov A G et al. *Prikl. Mat. Tekhn. Fiz.* (2) 86 (1982)
23. Glushak B L et al. *Zh. Eksp. Teor. Fiz.* **96** 1301 (1989) [*Sov. Phys. JETP* **69** 739 (1989)]
24. Al'tshuler L V et al. *Prikl. Mat. Tekhn. Fiz.* (2) 3 (1981)
25. Trunin R F et al. *Zh. Eksp. Teor. Fiz.* **102** 1433 (1992) [*Sov. Phys. JETP* **75** 777 (1992)]
26. Trunin R F et al. *Zh. Eksp. Teor. Fiz.* **103** 2189 (1993) [*Sov. Phys. JETP* **76** 1095 (1993)]
27. Trunin R F *Usp. Fiz. Nauk* **164** 1215 (1994) [*Phys. Usp.* **37** 1123 (1994)]
28. Kalitkin N N, Kuz'mina L V, Preprint IPM Akad. Nauk. SSSR No. 35 (Moscow, 1975)
29. Kopyshev V P *Chislennye Metody Mekhaniki Sploshnoĭ Sredy* **8** (6) 54 (1977) [Numerical Methods in Mechanics of Continua]
30. Trunin R F et al. *Teplofiz. Vys. Temp.* **32** 786 (1994)
31. *LASL Shock Hugoniot Data* (*Los-Alamos Series on Dynamic Material Properties*) (Ed. S P Marsh) (Berkeley, Los Angeles, London: Univ. California Press, 1980)